IVYSPRING INTERNATIONAL PUBLISHER

International Journal of Medical Sciences

2020; 17(7): 844-858. doi: 10.7150/ijms.41805

Review

Nano-scientific Application of Atomic Force Microscopy in Pathology: from Molecules to Tissues

Tony Mutiso Kiio and Soyeun Park✉

College of Pharmacy, Keimyung University, 1095 Dalgubeoldaero, Daegu 42601, Republic of Korea.

✉ Corresponding author: Soyeun Park, E-mail: sypark20@gmail.com. Tel.: +82-53-580-6654.

Received: 2019.11.05; Accepted: 2020.02.26; Published: 2020.03.15

Abstract

The advantages of atomic force microscopy (AFM) in biological research are its high imaging resolution, sensitivity, and ability to operate in physiological conditions. Over the past decades, rigorous studies have been performed to determine the potential applications of AFM techniques in disease diagnosis and prognosis. Many pathological conditions are accompanied by alterations in the morphology, adhesion properties, mechanical compliances, and molecular composition of cells and tissues. The accurate determination of such alterations can be utilized as a diagnostic and prognostic marker. Alteration in cell morphology represents changes in cell structure and membrane proteins induced by pathologic progression of diseases. Mechanical compliances are also modulated by the active rearrangements of cytoskeleton or extracellular matrix triggered by disease pathogenesis. In addition, adhesion is a critical step in the progression of many diseases including infectious and neurodegenerative diseases. Recent advances in AFM techniques have demonstrated their ability to obtain molecular composition as well as topographic information. The quantitative characterization of molecular alteration in biological specimens in terms of disease progression provides a new avenue to understand the underlying mechanisms of disease onset and progression. In this review, we have highlighted the application of diverse AFM techniques in pathological investigations.

Key words: atomic force microscopy; adhesion properties; disease diagnosis; morphology; mechanical compliance; molecular recognition

Introduction

AFM has emerged as a powerful nanoscopic platform to investigate various biological systems due to its applicability in physiological conditions. Unlike other scanning probe microscopic tools, AFM can be operated under physiological conditions. In addition to its sub-nanometer resolution and pico-newton force sensitivity, AFM is capable of recognizing single molecular events, compositional changes, and intercellular interactions occurring in heterogeneous biological systems during disease progression (Fig. 1) [1,2]. Many pioneer studies have investigated the possibility of utilizing AFM as a nano-diagnostic tool to establish unbiased quantitative assessment rubrics to monitor pathological conditions [3]. Comparative studies between healthy and pathologic specimens were performed using AFM. Nanoscopic structures, mechanical properties, and single molecular events were directly observed in cells and tissues via a minimally invasive surgical intervention [4].

Diseases usually evolve as a result of unwanted morphological alterations. In order to develop therapeutic interventions, it is important to identify the causes of disease-related phenotypes. AFM is capable of revealing disease-related structural changes [5,6]. It obtains topographic images based on the interatomic potential between the AFM probe and the samples. As the probe scans across the sample surface, the interatomic potentials move the cantilever in the perpendicular direction in order to keep a probe-sample interaction force constant. According to the cantilever's movement, the topography reflecting the contours of the sample surface is generated [7,8].

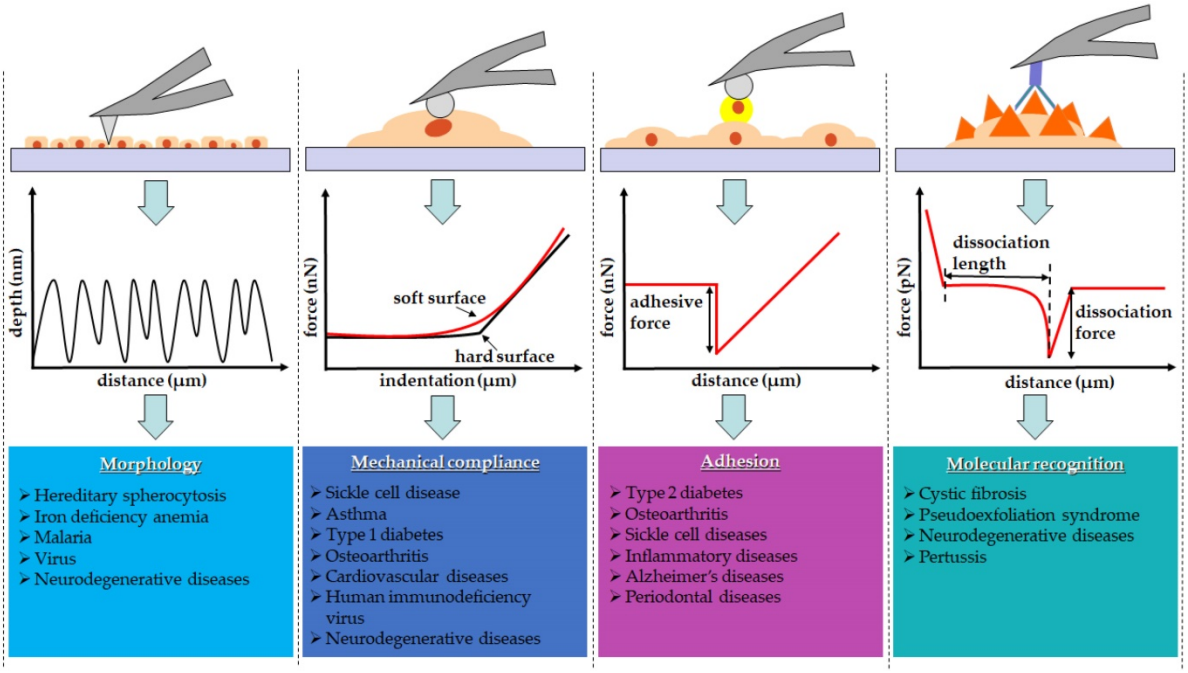

Figure 1. Various AFM-based techniques adapted to investigate biological specimens. The schematic drawings of an experimental technique and a corresponding line scan or force curve were illustrated for each experimental technique.

In addition, AFM as a nano-indenter is used to measure the mechanical compliances of biological samples. Cells actively reorganize their internal structure, leading to the alteration of their mechanical properties [9,10]. Many studies reported changes in the mechanical compliances of cells and tissues as pathologic manifestation [11,12]. The simple indentation of the AFM probe onto the sample yields a force-distance curve [13]. By analyzing the obtained force-distance curve using mathematical models, the mechanical compliances, *i.e.*, elastic moduli, were accurately determined. The Hertz model has been the most widely utilized mathematical model for this purpose. The mathematical models modified from the Hertz model have also been adapted in order to resolve the issues raised by the heterogeneous nature of biological samples [14-16].

Cell adhesion is essential in biological processes including cell proliferation, migration, and fate [17]. The adhesive strength of cells varies with substratum, topography, and chemo-mechanical properties surrounding the cellular microenvironment. Especially, the molecular composition and the mechanical properties of the extracellular matrix play a key role in cell spreading and migration [18]. Adhesion force is characterized by AFM-based pull-off force measurements in which the AFM probe approached a surface and then subsequently retracted. The pull-off force is defined as the maximum attractive force during the retraction of the tip from the surface [19, 20]. Pioneer studies have provided insight into disease-associated alterations in the cell-cell adhesion molecules expressed on the cell surfaces. For instance, the adhesion of ICAM-1, VCAM-1 and integrin VLA-4 on endothelial cells and monocytes is known to be a major contributor to determine the fate of inflammatory diseases [21-23]. The microbial adhesion on the enamel surfaces causes periodontal infection such as dental caries and cavities [21]. Moreover, metal ions such as zinc (II) and copper (II) are implicated with increased aggregation of the Aβ peptide into toxic oligomers, accelerating the pathogenesis of Alzheimer's disease [22,23]. Thus, the AFM- based studies attempted to investigate whether the disruption of the cell-cell/ substrate adhesions affects the progression of these diseases [24-28].

The quantitative characterization of intermolecular interaction is essential for a profound understanding of biological processes [29]. AFM probe functionalized with antibodies were utilized to recognize the antigenic sites on the surface of the cell membrane [30]. The extension lengths and the rupture forces were measured from the force-distance curves obtained while the probe retracted from the sample. They reflect the specific binding forces between the antibody attached on the AFM probe and the antigens on the cell surface. The map recognizing these specific binding forces refer to the molecular recognition imaging technique using the AFM. Using this technique, one can recognize antigenic sites on the cell membrane [31]. A variety of biosystems have been investigated by simultaneously obtaining topography and molecular recognition image. Molecular

interactions with high specificity including antigen-antibody, DNA aptamers, and ligand-receptor pairs have been utilized for this purpose [32,33]. The AFM molecular recognition imaging techniques were utilized to investigate the pathologic conditions such as cystic fibrosis, pseudoexfoliation [34], cystic fibrosis [35], pertussis [36] and neurodegenerative diseases [37], which were known to involve alterations in the molecular composition of cell membrane.

Many diseases display numerous pathophysiological modifications including structural or compositional changes, which can be used as diagnostic or prognostic markers [38-41]. AFM has been adapted to investigate such pathophysiological modifications to understand the underlying mechanism of various pathologic conditions. To do this, it is required to obtain biological specimens including blood samples and surgical specimens from patients and healthy volunteers in the clinical setting. For example, erythrocyte cells were isolated from blood samples in order to investigate hereditary spherocytosis, iron deficiency anemia, sickle cell disease, and type 2 diabetes using AFM [27,42-46]. In addition, it is relatively easy to obtain tissue samples from asthma patients for AFM studies because bronchial tissues can be collected through routine bronchoscopy [47]. However, studies on some diseases require more painful procedures for specimen collection. For instance, in order to investigate osteoarthritis, it is required to isolate chondrocyte cells from human articular chondrocytes tissues [48,49], and more rigorous surgical approach is required to obtain tissue samples from animals. Human tissues discarded from surgical procedures are also used in AFM studies. Islet tissue was surgically obtained from mice pancreas for AFM study on type 1 diabetes [50]. Similarly, human lens harvested from patients during cataract surgery was used for AFM study on pseudoexfoliation syndrome [51].

In this review, we address the potential of AFM as a clinical diagnostic tool to detect the pathological changes associated with various diseases. So far, there have been advances in the use of AFM for cancer diagnosis and prognosis. In our previous publications, we addressed various aspects of AFM applications in cancer biology [52]. However, in this review, we have focused on other diseases apart from cancer.

Morphology

Since live erythrocytes were first imaged by AFM, there has been a remarkable breakthrough in cell imaging with AFM under physiological conditions [53]. Many AFM studies have been performed on various kinds of cells under controlled pH and temperature in liquid environments, to avoid unfavorable distortion in images. AFM images provide detailed morphological features such as size, shape and surface topography at sub-nanometer resolutions [54-57]. In addition, it provides information on cellular architectures such as structural, conformational, and constitutional information of cytoskeletal proteins and membrane lipids [58-61]. During pathological progression, cells often undergo morphological modulations. Due to its high resolution, AFM can visualize early subtle changes in cell morphology prior to significant pathological conditions beyond the detection limit of other microscopic investigations. Morphological changes can also be observed with AFM shortly after therapeutic intervention, and thus, therapeutic efficacy can be evaluated by AFM images.

A healthy erythrocyte has a biconcave disk shape with a very shallow center. A disorder in erythrocytes can be detected by monitoring the shape, size, membrane proteins, number, and hemoglobin contents [62,63]. Abnormalities found in erythrocytes are pathological indicators in many diseases such as hereditary spherocytosis (HS) [64], anemia [65], and malaria [66]. Physicians clinically diagnose anemia by measuring the number of erythrocytes and the amount of ferritin — an iron-containing protein in the blood [67]. Clinical guideline for the diagnosis of HS also recommends close monitoring of erythrocytes abnormality. To diagnose diseases associated with abnormal erythrocytes, hematocrit, osmotic fragility, and direct anti-globulin tests are usually carried out to measure the volume as well as the fragility of erythrocytes and determine the antibodies attached to erythrocytes [64,67]. Nevertheless, the aforementioned tests lack specificity and often lead to false positive results, predicting a wide spectrum of clinical disorders [64,66-68].

Several studies suggested that AFM images can serve as a diagnostic alternative tool with higher specificity and accuracy as summarized in Table 1 [54,55,69]. HS is one of the hemolytic disorders caused by congenital defects. Anemia, jaundice, and splenomegaly are clinical symptoms experienced by HS patients. AFM study identified the morphological hallmark in HS patients as small spheroidal erythrocytes with poorly-organized membrane lattice, decreases in height, peak-to-valley distances, and surface roughness [42]. Surgical intervention, such as splenectomy, is a therapeutic strategy that has been adopted to relieve HS symptoms. A comparative study using AFM was performed to evaluate the efficacy of splenectomy on HS patients [42]. Interestingly, although this surgical intervention was

effective as a remedy for hemolytic anemia and other symptoms found in HS patients, AFM study revealed that there was no morphological restoration of erythrocytes, suggesting the need for a fundamental therapeutic intervention such as allogeneic hematopoietic stem cell transplantation. From the morphological point of view, the pathologic erythrocytes looking different from healthy ones were called elliptocytes appearing in the shape of ovals or elongated rods. AFM images obtained from erythrocytes in patients with iron deficiency anemia showed significant aggregation of membrane proteins. Further deformation was observed on the cell surface showing the swelling of the cell center deviated from the normal biconcave shape [43]. From the study, complete restoration of the morphology of erythrocytes during treatment was proposed as a criterion to determine the appropriate time for treatment termination.

The most remarkable superiority of AFM images over other microscopic images is that they are capable of visualizing cellular morphology and the ultramicroscopic structures of the cell membrane. Traditional diagnosis of malaria relies on the microscopic examination of malaria parasitemia from stained blood samples smeared on glass slides [66]. In this microscopic diagnosis, low resolution and dry conditions make it difficult to distinguish malaria parasites from similar species. Consequently, false-positive results, late detection, or absence of standardization in the diagnosis of malaria parasitemia have resulted in increased mortality [66,68,70,71]. Epidemiological and molecular studies have reported that the spectrin-based cytoskeleton of erythrocytes is strongly associated with malaria pathogenesis [72,73]. Spectrin is a cytoskeletal protein on the plasma membrane of erythrocytes, which forms a mesh structure by associating with actin filaments, and thus maintains plasma membrane integrity. During the progression of malaria pathogenesis, the erythrocytes infected by the human malaria parasites, *Plasmodium falciparum,* are expected to undergo substantial changes in membrane integrity and deformability for effective transmission to mosquitoes [74-76]. Indeed, an AFM study confirmed the appearance of "knobs", the assembly of adhesive proteins on the membrane of infected erythrocytes, the elongation of spectrin filaments, and the enlarged spectrin mesh during the progression from the ring (early) and trophozoite (growing) stages to the schizont (dividing) stages [77]. Recent AFM study, involving coarse-grained molecular dynamics simulation, explicitly showed the reversible modulation of the spectrin-actin network [78].

An AFM study investigated changes in the morphology of host cells during viral infection. The virus entered the host cells through physical adhesion and engulfment to the host cells. The inevitable morphological and mechanical modulations of the host cells were anticipated during the viral infection. A significant protrusion and softening of the cell membrane, attributed to the viral infection, were directly revealed by the AFM topographic images [79]. The study reported that the different sizes of membrane protrusion were associated with exocytosis of the protein structures and the progeny virus.

Table 1. Morphological changes observed by the AFM topography during disease onset and progression

Disease	Cells	Imaging condition	Changes from healthy to pathological conditions	Reference
Hereditary Spherocytosis	Human Erythrocytes	IC (Live cells)	Decrease in L from 6.51 ± 0.27 nm to 5.92 ± 0.27 nm and in W from 6.22 ± 0.15 nm to 5.81 ± 0.12 nm Increase in height from 586 ± 120 nm to 1,644 ± 34 nm Decrease in Rp–v from 1,272 ± 48 nm to 1,058 ± 155 nm Decrease in Ra from 287 ± 44 to 215 ± 6	[42]
Iron deficiency anemia	Human Erythrocytes	CM (Dead cells)	Increase in protein particle size from 8 nm to > 140 nm Increase in r from 1.01 ± 0.06 to 1.52 ± 0.47 Decrease in H from 1,729 ± 39 nm to 1,518 ± 72 nm Increase in h from 41 ± 6 nm to 403 ± 43 nm Decrease in Rp–v from 1,605 ± 29 nm to 1,154 ± 88 nm Increase in Ra from 582 ± 26 nm to 1,227 ± 91 nm	[43]
Malaria	Cultured Erythrocytes	CM and IC (Dead cells)	Increase in spectrin length from 48 ± 7 nm at ring stage to 64 ± 9 nm at early and middle trophozoite stage, 69 ± 10 nm at late trophozoite stage, and 75 ± 11 nm at schizont stage	[77]
	Human red blood cells	IC (Dead cells)	Changes in spectrin length from 61 ± 14 nm at trophozoites stage, to 62 ± 8 nm at gametocytes stage, and 42 ± 12 nm at stage V gametocytes	[78]
Pox virus	Kidney cells	Live cells	Exocytosis of protein structures: 10–100 nm in diameter Exocytosis of progeny virus: 200–300 nm in diameter	[79]
Neurodegenerative diseases	$A\beta_{1-42}$ fibril	HSI	Observed two growth modes of $A\beta_{1-42}$: One producing straight fibrils and another producing spiral fibrils	[83]

Abbreviations: $A\beta_{1-42}$: amyloid β peptide; CM: contact mode; h: valley height; H: peak height; HSI: high-speed imaging; IC: intermittent Contact; L: length; Ra: surface roughness; Rp–v: peak-to-valley distance; r: ratio of length to width; W: width.

Despite the numerous advantages, AFM imaging technique is limited by time resolution; it usually takes about 5 min to obtain a single frame of image. To overcome this problem, high-speed atomic force microscopy (HS-AFM) was invented [80]. The first generation of HS-AFM could capture the images of moving proteins at a rate of 80 ms per frame [80]. With recent advances, the real-time imaging of biological process at a molecular level has been achieved. As an example, myosin V walking along actin filaments was successfully visualized by HS-AFM [81,82]. Indeed, the fast-scan ability of HS-AFM seems very beneficial in the monitoring of the dynamic changes of biological specimens during pathological progression of diseases. An interesting study using HS-AFM has been reported by Watanabe-Nakayama *et al* [83]. Using HS-AFM, they successfully monitored the dynamic process of fibril formation and elongation of amyloid β-protein (Aβ), a key pathogenic agent in neurodegenerative diseases such as Alzheimer disease. Amyloid fibril accumulation is associated with numerous neurodegenerative diseases [84-93]. However, the mechanisms by which Aβ accumulation in the brain leads to neurodegeneration remain unclear. The clarification of the fibrillation mechanism, the structural features of the amyloid fibrils, and their physical and mechanical properties are expected to unveil the roles of amyloid fibrils in the progression of a range of conditions from mild cognitive impairments to Alzheimer's disease [94]. HS-AFM images show two different growth modes of Aβ, one producing straight fibrils and the other producing spiral fibrils. The switch between two different growth modes was suggested to be a key step in determining Aβ polymorphisms associated with the pathogenic condition.

The AFM was also adapted to witness the effect of compounds or drugs inducing nanoscale morphological modification in single cells. For instances, glutaraldehyde is a common chemical fixative used to preserve cells/tissues for the electron microscopy. Shibata-Seki *et al.* investigated the effect of chemical fixation of glutaraldehyde on corneal endothelial cells using the AFM. They found that the treatment of glutaraldehyde resulted in shrinkage of the endothelial cells owing to the evaporation of water [95]. Glycans play a key role in physiological and pathological processes by mediating cell-cell and cell-ECM interactions. Glycosylation of the biomaterials influences cell fate such as proliferation, differentiation, and functionality. Figuereido *et al.* used AFM to investigate the biocompatibility of neoglycosylated films on human SYSH-SY5Y neuroblastoma cell lines [96]. The AFM topographic images showed that the neoglycosylated collagen films exhibited well-defined fibrillary structures, while untreated control had amorphous structures. Furthermore, the human SH-SY5Y neuroblastoma cells had comparable biocompatibility to the neoglycosylated collagen films. Their results suggested that the morphological alteration of the neoglycosylated collagen could modulate the inter-molecular and inter-fibrillar interactions of the triple-helical domain of the collagen films resulting in improved biological activity. Antimicrobial peptides are a promising class of antimicrobials that exhibits activity against antibiotic-resistant bacteria, parasites, and viruses. Fantner *et al.* used HS-AFM to monitor real-time morphological modification induced by the antimicrobial peptide CM15 on living *Escherichia coli* bacteria cells at a nanoscale resolution. They found that the cell surface changed from smooth to being corrugated after treating with CM15 [97].

AFM has been used to monitor the morphological distortion of cells at nanometer resolution. The high-resolution images provided more quantitative and bias-free diagnostic means beyond the conventional diagnostic assays. Although the use of AFM imaging technique in the observation of biological samples has its own drawbacks, it offers an invaluable potential as a diagnostic tool especially when combined with existing diagnostic tools [98].

Mechanical compliance

Many diseases are inherently accompanied by mechanical alteration of tissues and cells. For instance, skin aging induces decrease in skin resilience, which is attributed to changes in the composition and organization of extracellular matrix [99]. Consequently, the mechanical properties of cells and tissues are important indicators of pathologic progression of diseases [100]. Mechanical compliance, also called softness, indicates the flexibility of tissues or cellular materials under external stress. The extent of mechanical compliance is often expressed as elastic moduli, *i.e.,* Young's moduli, which can be calculated from stress-strain relation. A high Young's modulus indicates a low mechanical compliance [101]. Over the past decades, various techniques have been developed to investigate the mechanical compliances of biological samples such as cells and tissues. These techniques include optical stretcher [102-105], micropipette aspiration [106], microfluidics [107], magnetic tweezers [108-110], and AFM [111-114]. Among these, AFM has been the most widely utilized in bio-mechanical assays [13,52,115-118].

A simple indentation experiment was carried out to determine the elastic moduli of samples. Some attempts were made to obtain both the storage and

loss moduli of biological samples by superimposing the oscillating motion on the probe while indenting the samples [113,115,119]. For the clinical applications of AFM techniques, there have been an increasing number of studies investigating tissues obtained from a minimally invasive surgical intervention such as biopsy [47,50,120]. One of the long-standing problems associated with probing tissues, in comparison with cells, is the technical difficulty associated with immobilizing tissue samples on hard substrates in liquid environments. To overcome this problem, a novel method was adopted for the efficient immobilization of tissues. Nanopillars of "bed of nails"-like approach to anchor pancreatic islet demonstrates an exemplary strategy to achieve proper immobilization of tissues [50]. In addition, comparative studies that evaluated changes in elastic moduli with regards to storage and buffer conditions have been carried out to establish the standard conditions for AFM nano-mechanical studies on tissues [47].

Table 2 summarizes AFM-based bio-mechanical reports on changes in elastic moduli attributed to disease onset and progression. Interestingly, while samples from diseases such as sickle cell disease and cardiovascular complications showed increase in Young's moduli compared to healthy samples, other samples from diseases such as asthma, osteoarthritis, and diabetes conversely showed reduced mechanical integrity.

Sickle cell disease is an inherited disorder caused by genetic mutation in the hemoglobin. AFM indentation experiments performed on human erythrocytes harvested from patients with sickle cell disease showed that pathological erythrocytes is about three times stiffer than normal cells [44]. The seven stranded polymer structure of hemoglobin S and changes in the affinity of spectrin and actin filaments were suggested to be responsible for the increased stiffness of sickled erythrocytes.

Mechanical stiffening has also been noted as a hallmark of cardiovascular complications [119,121]. A recent AFM study directly observed a significant increase in the elastic moduli of ventricular tissues freshly harvested from mice with pressure overload-induced cardiac hypertrophy [121]. Cardiac hypertrophy, a leading cause of cardiac complication-induced death, is characterized by the abnormal enlargement and thickening of the myocardium. The study also reported that increase in the elastic moduli of hypertrophic myocardium enhances the production of vascular endothelial growth factor through PI3K/Akt signaling pathway, thus facilitating angiogenesis during the progression of cardiac hypertrophy to heart failure. The mechanical stimuli from the stiffened matrix were found to be mediated by talin 1 and integrin β1. The findings of the study provided information not only on the direct quantification of mechanical changes in the myocardium but also on novel pharmacological interventions to slow down the detrimental progress of cardiac hypertrophy. Moreover, age-related aortic stiffening, another cause of heart failure, was quantitatively evaluated by an AFM-based bio-mechanical assay [119]. The study was unique because frequency modulated atomic force microscopy (FM-AFM) was used to determine both the storage and loss moduli in localized regions. The study reported an age-induced elevation in elastic moduli, which was more prominent in the inter-lamellar regions than in the lamellar regions. Inter-lamellar regions are composed of complex meshwork of collagen fibers, elastin fibers, and smooth muscle cells, of which major rearrangements occurred due to aging, and thus their mechanical alterations were more severe than those of other regions.

Table 2. Alteration in mechanical compliance of cells and tissues revealed by the AFM studies during disease progression

Pathological changes in E	Disease	Samples	Changes from healthy to pathological condition	References
Increase	Sickle cell disease	Human erythrocytes	1.10 ± 0.40 kPa to 3.0 ± 1.09 kPa	[44]
	Cardiac hypertrophy	Mice ventricular tissues	13.5 ± 0.665 kPa to 34.1 ± 1.37 kPa	[121]
	Aging	Sheep aorta	Lamellar region: Young (36 ± 2.22 Kpa) to old (63 ± 2.95 Kpa) Inter-lamellar region: Young (25 ± 3.39 Kpa) to old (63 ± 2.76 kPa)	[119]
	Aging	Mice articular cartilage	23 ± 1.9 kPa at 6 months to 41 ± 2.9 kPa at 12 months	[125]
Decrease	Osteoarthritis	Human chondrocytes	0.0960 ± 0.009 N/m to 0.0347 ± 0.005 N/m	[48]
		Human articular cartilage	83 Kpa to 5.6 kPa	[125]
		Mice articular cartilage	38 ± 3.4 kPa at 6 months to 20 ± 3.4 kPa at 12 months	
		Rabbit chondrocytes	1.43 ± 0.45 Mpa to 0.16 ± 0.08 Mpa	[49]
	Type 1 diabetes	Mice islets tissue	~3 kPa to ~284 Pa	[50]
	Asthma	Human bronchial tissue	Lower stress: 14.6 ± 8.2 kPa to 7.7 ± 4.0 kPa Higher stress: 3.5 ± 1.8 kPa to 1.8 ± 1.0 kPa	[47]
	HIV-1 virus	Virus particles	Immature HIV-1 virus: 0.93 GPa Mature HIV-1 virus: 0.44 GPa	[128]
	Nerve injury	Mice neurons	Softening of growth cone about 20 to 40 %	[131]

Abbreviation: E: elastic modulus.

Age-related mechanical degradation of human chondrocytes has been reported by an AFM study [48]. In this study, it was observed that old chondrocytes had three-fold lower stiffness than normal counterparts. There was a similar observation with sodium nitroprusside (SNP)–induced chondrocyte apoptosis, a typical osteoarthritis model; SNP-treated chondrocytes showed remarkable decrease (90%) in elasticity [49]. Chondrocytes are embedded in the extracellular matrix which is composed of collagens, proteoglycans, and glycoproteins to form articular cartilage. The aging of the articular cartilage results in cartilaginous degeneration such as osteoarthritis [122]. The mechanical disintegration observed in old chondrocytes is strongly associated with distorted macromolecular framework attributed to the aging process, leading to the damage or death of chondrocytes [123,124]. Strikingly, the mechanical disintegration of aged chondrocytes is seemingly contrary to the age-dependent mechanical modulation of human articular cartilage. Stolz *et al.* reported the age-dependent-stiffening of articular cartilage with progressive decrease in glycosaminoglycan contents [125]. However, the elastic moduli observed in osteoarthritis patients confirmed the progressive softening of articular cartilage. The age-dependent stiffening of human articular cartilage is overruled by the progressive softening found in osteoarthritis. Again, the mechanical softening of articular cartilage is attributed to the disintegration of collagen meshwork. In addition, such mechanical modulation of articular cartilage was apparent not at micrometers but at nanometers of indentation depth. This requirement of nano-manipulation suggests that the AFM-based indentation technique might serve as a pre-symptomatic diagnostic tool for osteoarthritis. A study has demonstrated that the elastic modulus determined by AFM indentation experiments can be utilized as a progressive disease marker during the treatment of osteoarthritis [49]. The study also reported the preventive effect of resveratrol on SNP–treated chondrocytes. Resveratrol is a polyphenol, derived from some fruits such as grapes, and an anti-inflammatory agent [49]. The elastic moduli, measured by AFM, showed that pretreatment with resveratrol prevents chondrocytes from undergoing SNP-induced mechanical disintegration. Immunofluorescent images revealed that such mechanical modulations resulted from the active reorganization of the actin cytoskeleton induced by resveratrol treatment.

It is also fascinating that AFM studies have also reported close correlation between inflammatory diseases, such as asthma, and the mechanical softening of tissues [47,50]. The mechanosensitive production of insulin from islets was confirmed by AFM-based nano-indentation experiments performed on transgenic DORmO mouse model of type 1 diabetes [50]. The study showed that autoimmune insulitis resulted in mechanically soft islets. The intraislet accumulation of hyaluronan prior to the onset of diabetes was considered as a major cause of such mechanical changes. Hyaluronan, a polymer in the extracellular matrix is highly hygroscopic, and thus, its increased accumulation promotes hydration and softening of tissues. Asthma is a hyper-responsive complication in the airway characterized by chronic inflammation. Structural remodeling of bronchial walls includes aberration in the extracellular matrix composition, increase in collagen type I, III, and V, as well as fibronectin, and decrease in collagen type IV [126,127]. Lately, AFM studies on tissues from bronchial biopsies reported lower elastic moduli in airway tissues collected from asthma patients than those in tissues collected from healthy volunteers [47]. Although the major determinants contributing to the reduced mechanical stiffness of bronchial tissues in asthmatic patients are yet to be determined, AFM nano-indentation has emerged as an early and quantitative diagnostic tool for asthma, a respiratory complication with various symptoms.

Remarkably, an AFM nano-indentation study has been conducted to investigate fundamental information required to fight against intractable diseases such as human immunodeficiency virus (HIV) infections and nerve injury. The study provided quantitative evidences to depict the mechanically switching behavior of HIV during the infection process [128]. A stunning switch between softening and stiffening behaviors took place from viral budding to viral entry into the host cells. More detailed investigation was conducted to address the mechanical stability of HIV-1 capsid using AFM, revealing the mechanical hardening of hyperstable mutants. Mutations modulating capsid stability are known to largely affect HIV infectivity. Similarly, AFM experiments were carried out to depict the fundamental mechanism of axonal degeneration due to nerve injury or compression. A state-of-the-art study combining microfluidics with AFM was performed to determine the threshold force required to compromise axonal survival after compression [129]. The study showed that rat hippocampal axons fully recovered axonal transport with no detectable axonal loss when compressed with pressure up to 65 ± 30 Pa for 10 min. Whereas, the dorsal root ganglia axons, which showed 20% lower elastic modulus than hippocampal axons, resisted pressure up to 540 ± 200

Pa. It was suggested that the integrity of axonal cytoskeleton mainly affects axonal fate after damage. AFM-based force spectroscopy, combined with fluorescence microscopy, has also been used to determine changes in neuronal stiffness during neurite outgrowth [130]. Fluorescence images indicated that the organization of microtubules is a major component associated with neuronal stiffness. In addition, the AFM study explicitly determined that the growth cones of axotomized neurons underwent mechanical softening during sciatic nerve injury [131]. Although it is too early to determine if AFM demonstrates diagnostic advantages for HIV and nerve injury, the obtained information from AFM studies would be crucial to the improvement of pharmacological interventions for the treatment or prevention of these intractable diseases.

Each of the aforementioned diseases has its own underlying mechanism that causes the corresponding mechanical alterations. Nevertheless, each disease generally involves the aberrant reorganization of actin cytoskeleton or the extracellular matrix. Depending on the extent of hydration, the organization and composition of the extracellular matrix or the actin cytoskeletal proteins are modulated during disease onset and progression, and changes in elastic moduli appear in two different directions of the stiffness spectrum as shown in Table 2. Even the reversible switching behavior was observed in HIV infection. As shown in osteoarthritis, the interplay between mechanical changes in cells and their microenvironments collectively affect the mechanical behavior of tissues during disease progression. Herein, we show that AFM-based biomechanical studies are promising in the early diagnosis of diseases because they are able to detect the pre-symptomatic changes in the mechanical properties of cells and tissues in many pathological conditions.

Adhesion properties

Cell adhesion plays an important role in cell communication and regulation. The mechanical interaction between a cell and its extracellular matrix (ECM) controls cellular behavior and functions. The alteration of cell adhesion can be a defining event for the onset of numerous diseases such as type 2 diabetes, neurodegenerative diseases, osteoarthritis, cardiovascular diseases and sickle cell anemia [132-136]. Tremendous efforts have been made to develop various techniques to quantitatively determine cell adhesion [137]. Recently, AFM has been extensively utilized to determine the adhesive properties of cells [31,135,136,138-141].

Simple studies using the AFM-based adhesion assay were performed to investigate bacterial adhesion on dental surfaces [28,142]. Bacterial adhesion is considered as a primary cause of periodontal diseases such as dental caries and cavities [143]. For more than half a century, the fluoride treatments of teeth have been carried out in order to prevent dental caries. An AFM study revealed that the reduced bacterial adhesion on enamel surfaces is a key factor associated with the cariostatic effect of fluoride treatment [142]. Furthermore, dental restorative materials such as composite resin Amelogen® and dental alloy often attract bacterial adhesions, resulting in the formation of secondary caries. AFM-based force spectroscopy evaluated the adhesion forces of cariogenic pathogens such as *Staphylococcus aureus* on dental restorative materials as shown in Table 3. The finding of the study suggested that surface roughness and free energy on initial staphylococcal adhesion forces are the main characteristics to be considered for dental restorative materials.

Table 3. Changes in adhesion properties revealed by the AFM studies during disease progression

Disease	Sample	Functionalization on the probe	Changes from healthy to pathological conditions	References
Type 2 diabetes	Human erythrocyte	None	Increase in AF from 200 ± 38 pN (young) and 420 ± 25 pN (old) to 510 ± 63 pN	[45]
Osteoarthritis	Human articular chondrocytes	None	Decrease in AF from 7 ± 3 nN to 2 ± 1 nN	[48]
Sickle cell diseases	Human red blood cells	Integrin $\alpha v\beta 3$	Increase in ICAM-4 AF after epinephrine treatment from 10.08 ± 0.85 % to 21.41 ± 2.27 %	[27]
Inflammatory diseases	Human T-leukemia Jurkat cells and HUVECs	Human junctional adhesion molecule-A antibody	Increase in DA of stimulated HUVEC center from $1 \times 10^{-16} \pm 0.42$ J to $3 \times 10^{-16} \pm 0.55$ J and junction from $1 \times 10^{-16} \pm 0.45$ J to $7 \times 10^{-16} \pm 0.58$ J	[154]
Alzheimer's disease	Cys-Aβ42	Aβ peptides	Increase in Aβ-Aβ affinity from 0.40 ± 0.16 mM without zinc to 7.50 ± 2.06 mM with zinc ions	[156]
Periodontal diseases	Human whole saliva and *Staphylococcus aureus* bacteria	*Staphylococcus aureus* bacteria	Cobalt-nickel-chromium for dental alloy AF: 5.9 nN Feldspathic ceramic AF: 7.7 nN Composite resin Amelogen® Plus AF: 7.8 nN Denture base polymer for dental prosthesis AF: 11.6 nN	[28]

Abbreviations: AF: adhesive force; DA: de-adhesion force; HUVEC: human umbilical vein endothelial cell; ICAM-4: intercellular adhesion molecule-4.

As summarized in Table 3, AFM-based adhesion assays investigate how various pathologic conditions lead to changes in the adhesion properties of cells. First, it has been shown that aging and diabetes increase the adhesion properties of erythrocytes [45]. Type 2 diabetes is a metabolic disorder with high sugar levels in the blood owing to insulin resistance or deficiency [144-146]. It has been postulated that high level of glucose in the blood enhances viscosity and aggregation in the membrane of erythrocytes. The increased adhesion properties of the erythrocytes of old people explains why elderly persons are more vulnerable to vascular diseases including diabetes. Remarkably, the increase in the adhesion properties of erythrocytes found in patients with type 2 diabetes were more significant than the changes observed in old healthy people.

Unlike the diabetes-induced changes in adhesion properties, some diseases such as osteoarthritis lead to decrease in the adhesion properties of cells [48]. Clinically, osteoarthritis (OA) is diagnosed with radiography [147]. Radiographic examination provides information on bony changes that occur during OA prognoses such as osteophyte formation, subchondral sclerosis, asymmetric joint space narrowing, subchondral cysts, and subluxation [147-151]. However, radiography diagnosis often provide a delayed or missed diagnosis of OA [152]. Thus, an AFM-based study was performed to investigate the prognoses of OA [48]. The study showed that the adhesion forces of OA chondrocytes were relatively low and distributed over a narrow range compared to normal chondrocytes (see Table 3). Furthermore, the study revealed a decrease in integrin β_1 mediated chondrocyte-ECM interactions in OA, implicating the perturbation of cell matrix in OA. The down-regulated expression of integrin β_1 in OA chondrocytes was observed as the main mechanism behind the reduced adhesion forces of OA chondrocytes.

The adhesions detected by bare AFM probe involve the collective interactions between the probe and various proteins on the cell membrane. It is not easy to determine which component among the various adhesion-mediating molecules is responsible for such modulated adhesions observed in diabetes and OA. There were attempts to adopt AFM-based single-molecule force spectroscopy (SMFS) in order to determine specific molecules mediating adhesions in pathologic conditions. The AFM-based SMFS detects single functional receptors on cells and the unbinding force between a receptor and the corresponding ligand. Several pathologic disorders such as sickle cell disease, inflammation, and autoimmune blistering skin disease were investigated using this AFM technique. The sickled red blood cells (RBCs) are known to show increase in adhesions to other RBCs and the endothelium. The enhanced adhesion of RBCs to the endothelium causes a delayed microvascular passage of deoxygenated RBCs, promoting sickling and entrapment of RBCs. Consequently, these series of events initiate vaso-occlusive episodes, which are characteristics of sickle cell disease. An AFM-based adhesion assay identified that increase in the binding events between intercellular adhesion molecule-4 (ICAM-4) and $\alpha_v\beta_3$ integrin results in the abnormal adhesion of sickled RBCs to endothelial cells [27]. The study also showed that ICAM-4 is activated by cyclic adenosine monophosphate-protein kinase A-dependent pathway [27]. The recruitment of leukocytes into injured tissues leads to the progression of inflammation [153]. In the beginning of inflammatory pathogenesis, leukocytes in the blood circulation adhere to vascular endothelial cells and migrate through endothelial cells into the interstitial space. Jaczewska *et al.* showed that the adhesion of Jurkat cells to stimulated HUVEC monolayers took place remarkably in junctional regions [154]. Furthermore, AFM adhesion mapping revealed that the redistribution of junctional adhesion molecule-A (JAM-A) along junctional regions plays a key role in mediating lymphocyte recruitment to the endothelium and subsequent transendothelial migration under inflammatory conditions. AFM adhesion study was also utilized to investigate the molecular signature of gap junctions associated with autoimmune blistering skin disease such as pemphigus vulgaris (PV) [155]. Desmosomal junctions are cadherin-based intercellular junctions in epithelial tissues and their disruption strongly correlates with the incidence of PV. The study revealed that the incubation of pathogenic antibodies with desmoglein 3 resulted in the disruption of intercellular adhesion and structural changes in human keratinocytes, leading to blister formation.

Furthermore, AFM-based adhesion study has been used to determine the effects of trace elements on the progression of neurodegenerative diseases. With trace metals such as copper and zinc, the aggregation and neurotoxicity of amyloid-β (Aβ) is significantly enhanced. The aggregation of Aβ is considered as a major cause of Alzheimer's disease. Recently, Hane *et al.* used AFM to characterize the kinetic and thermodynamic parameters of the dissociation of an Aβ dimer in the presence of copper and zinc ions [156]. Their results demonstrated that while copper at a nanomolar concentration did not alter the single molecule affinity of Aβ-Aβ, zinc at the nanomolar concentration reduced the Aβ-Aβ affinity.

Overall, different studies have indicated that altered cell adhesion is a defining event in the onset and progression of various pathological conditions. The accurate determination of cell adhesion is critical information for the diagnosis and prognosis of diseases. We believe that molecular signatures revealed by AFM-based force spectroscopy provide valuable information not only for the diagnosis of different diseases but also for the development of therapeutic strategies.

Molecular recognition imaging

The cell membrane is composed of interdependent species of molecules, molecular groupings, and supramolecular entities, which play a crucial role in cell functions such as cell adhesion, cellular communication, tissue development, inflammation, tumor metastasis, and microbial infection [1,157]. Some molecules act as receptors and others as sensors controlling the important cellular processes [158,159]. The malfunction of membrane proteins often results in the onset of diseases. Many diseases including pseudoexfoliation [34], cystic fibrosis [35], neurodegenerative diseases [37], and pertussis [36] are associated with alterations in the molecular composition of cell membrane. Consequently, many therapeutic drugs target the human membrane proteins [160]. Previously, cryo-electron microscopy [161], photoactivated localization microscopy [162], and X-ray crystallography [163] have been used to obtain the molecular structures of the cell membrane. Nevertheless, the images obtained from these techniques provided distorted information due to the pretreatment of the target molecules [2]. Thus, the emergence of AFM offers an exciting methodology to monitor membrane proteins in near-native physiological conditions.

Molecular recognition imaging technique using AFM combines molecular recognition with force microscopy [32,164]. The obtained images successfully show the chemical composition of the sample as well as its topographical structures. This technique allows molecular recognition with concentrations below the detection limits of current technologies such as enzyme-linked immunosorbent assay, mass spectroscopy, and protein microarray [165, 166]. In order for AFM to detect specific targets, the AFM probe has to be functionalized with a molecule of high affinity [33,167]. The force applied to break the chemical bond between the probe and the target molecule is quantitatively determined from the force-distance curve [168-170]. Previous studies have demonstrated that a silicon nitride cantilever tip functionalized with DNA aptamers and cyclo-RGD peptides is able to detect their cognate *a*-thrombin, IgE molecules, and integrin $\alpha_5\beta_1$ with high accuracy upto ~90 % [33,171].

The cystic fibrosis transmembrane conductance regulator (CFTR) is a channel localized on the apical membrane of the epithelial cells lining exocrine glands. The CFTR maintains the salt and water balance in the epithelium and regulates cell volume [172,173]. CFTR dysfunction results in a severe disease known as cystic fibrosis (CF), characterized by impaired epithelial transport in the respiratory system, liver, and pancreas. The prevalent alteration is the deletion of the amino acid phenylalanine at position 508, subsequent misfolding, impaired trafficking to the membrane, and the reduced number of CFTR on the plasma membrane [174-176]. Clinically, a sweat test is used to measure the level of the chloride ions in sweat via quantitative coulometric test or chloride titration test. However, the sweat test method is highly unreliable because of insufficient production of sweat [177]. Ebner *et al.* used the AFM molecular recognition imaging technique to investigate CFTR in erythrocytes membrane at the single-molecule level [46]. While the normal human erythrocytes have high permeability to chloride [178, 179], the erythrocytes of CF patients with the F508del mutation showed about 30 % decrease in CFTR on the plasma membrane.

The AFM molecular recognition imaging technique was also adapted for the monitoring of protein aggregation on the human lens capsule [180]. Pseudoexfoliation syndrome (PEX) is charaterized by the deposition of whitish-grey extracellular fibrins in the anterior lens capsule, leading to irreversible blindness [181-183]. PEX is usually diagnosed by slit lamp using biomicroscopy [184]. However, biomicroscopy technique cannot provide information on protein changes that cause the onset of PEX, to facilitate the development of treatment modalities. The AFM molecular recognition images obtained by Creasey *et al.* identified the localized distribution of clusterin, one of the proteins implicated in PEX, while indicating that clusterin did not follow a specific distribution pattern observed on normal lens capsules [51]. The distribution pattern occurred due to the aggregation of misfolded proteins in PEX, leading to a chaperone response by clusterin. This investigation shows the feasibility of the use of AFM molecular recognition imaging technique to detect pathological alteration of biological tissues.

Interestingly, the nicotinic acetylcholine receptor (nAChR) on neurons from the ventral respiratory group was monitored by AFM molecular recognition imaging technique [185]. nAChR is a member of the ligand-gated ion channels in the central and peripheral nervous systems [186]. The functional

alteration in the α7 nAChRs has been implicated in the abnormal function of cells such as cell replication and differentiation, axonogenesis/synaptogenesis, as well as synaptic function and behavior [186, 187]. AFM probe was conjugated with anti-α7 subunit nAChR antibody, which interacts with the surface of NK1-R positive neurons. Acute exposure to nicotine caused an 80% decrease in the binding ability of nAChR antibody to the α-7 subunit in a dose-dependent manner. The study suggested that nicotine exposure reduced the binding probability of α-7 subunit-containing nAChRs, which correlated with the loss of nicotinic receptor function.

AFM molecular recognition technique has been extended into the study of medically important microbes. Pertussis is a toxin-mediated disease; *Bordetella pertussis* attaches to the cilia of the respiratory epithelial cells and secrets exotoxin. The secreted exotoxin incapacitates the cilia and results in the inflammation of the respiratory tract, which interferes with the clearing of the pulmonary secretion [188]. Bacteria adhesion is the most significant step in the development of bacteria infection. Pertactin, fimbriae, and filamentous haemagglutinin adhesin (FHA) proteins interact with different components of the respiratory epithelium to facilitate the attachments of the cells. FHA participates in the first step of adhesion through recognition domains by adhering to respiratory epithelial cells and macrophages [188-190]. In the clinical field, polymerase chain reaction is used for the detection of DNA sequences of *B. pertussis* [191]. AFM-based force spectroscopy assay was performed to obtain information about the localization and distribution of FHA-mediated adhesions in *B. pertussis* [192]. The force strength of the recognition events ranged from 50 pN to 900 pN. Cluster and nearest neighbor analysis revealed that the amount of cluster diminished during the time-lapsed imaging but the size of connected clusters markedly increased. It was shown that the active clustering of bacterium nanodomains on the cell membrane is a crucial step in bacterial infection. The study successfully demonstrated the application of AFM-based molecular recognition imaging technique in monitoring the spatio-temporal rearrangements of adhesins at the molecular level. The obtained information might contribute to understanding the basic molecular mechanisms through which bacterial pathogens cause infectious diseases.

Here, we understand that AFM molecular recognition imaging technique is widely utilized in the imaging of biological specimens including cells, tissues, and bacteria. It is demonstrated that this technique is capable of nanoscale imaging resolution and time-lapsed imaging ability. In addition, AFM provides highly reproducible, specific, and efficient molecular detection, and consequently, alteration in tissue and cell structures under pathological condition can be closely monitored. The detection of antigens is also more efficient without the lengthy preparation procedures. We anticipate that molecular recognition techniques would be very useful in the development of therapeutic modalities for various diseases.

Conclusion

In this review, we address the basic techniques of AFM, which have been widely utilized in the detection of pathological conditions. The increasing number of studies adapting AFM as a vital tool in the study of various pathological conditions indicates the intense scientific awareness of its potential. The nanoscale imaging capability has made it possible to detect morphological changes associated with diseases such as hereditary spherocytosis, iron deficient anemia, malaria, and neurodegenerative diseases. Accurate determination of cell/tissue stiffness has improved the early diagnosis of diseases such as sickle cell anemia, asthma, type 1 diabetes, osteoarthritis, cardiovascular diseases, and HIV infection. AFM can also be utilized to quantify the adhesion properties of cells. Diseases such as type 2 diabetes, osteoarthritis, sickle cell diseases, inflammatory diseases, Alzheimer's diseases, and periodontal diseases have been monitored in terms of adhesion properties. The molecular recognition imaging technique has revolutionized exploration of biological specimens at a single molecule level. Remarkably, this technique is a unique force spectroscopic tool which enables us to monitor the spatial distribution of chemical heterogeneity with the nanometer precision. Specific single molecule interactions include an antigen-antibody and a ligand-cell surface receptor bond. These interactions are prevalent in numerous biological processes such as immune response, genome replication and transcription, and infection. Interestingly, molecular recognition imaging techniques, using antibodies and antigens of interest, expand the application of AFM in pathologic investigations with a high degree of sensitivity and specificity. Cystic fibrosis, pseudoexfoliation syndrome, neurodegenerative diseases, and whooping cough have been studied using AFM-based molecular recognition imaging techniques. We expect that the diverse aforementioned AFM techniques would make a tremendous improvement in clinical studies. The molecular information obtained from AFM would facilitate early diagnosis of diseases before they

progress to complications which cannot be treated by the current therapeutic modalities.

Abbreviations

Aβ: amyloid β-protein; $A\beta_{1-42}$: amyloid β peptide; AF: adhesive force; AFM: atomic force microscopy; CF: cystic fibrosis; CFTR: cystic fibrosis transmembrane conductance regulator; CM: contact mode; DA: de-adhesion force; E: elastic modulus; ECM: extracellular matrix; FHA: filamentous haemagglutinin adhesin; FM-AFM: frequency-modulated atomic force microscopy; h: valley height; H: peak height; HIV: human immunodeficiency virus; HS: hereditary spherocytosis; HSI: high-speed imaging; HUVEC: human umbilical vein endothelial cell; IC: intermittent contact; ICAM-1: intracellular adhesion molecule 1; ICAM-4: intercellular adhesion molecule-4; JAM-A: junctional adhesion molecule-A; L: length; nAChR: nicotinic acetylcholine receptor; OA: osteoarthritis; PEX: pseudoexfoliation syndrome; PV: pemphigus vulgaris; R: ratio of length to width; Ra: surface roughness; RBCs: red blood cells; Rp–v: peak-to-valley distance; SMFS: single-molecule force spectroscopy; SNP: sodium nitroprusside; VCAM-1: vascular cell adhesion molecule-1; VLA-4: very late antigen-4 integrin; W: width.

Acknowledgments

This research was supported by Keimyung University Research Grant of 2018.

Competing Interests

The authors have declared that no competing interest exists.

References

1. Hinterdorfer P, Garcia-Parajo MF, Dufrene YF. Single-molecule imaging of cell surfaces using near-field nanoscopy. Acc Chem Res. 2012; 45: 327-36.
2. Li M, Dang D, Liu L, Xi N, Wang Y. Imaging and force recognition of single molecular behaviors using atomic force microscopy. Sensors (Basel, Switzerland). 2017; 17.
3. Carvalho FA, Connell S, Miltenberger-Miltenyi G, Pereira SV, Tavares A, Ariens RA, et al. Atomic force microscopy-based molecular recognition of a fibrinogen receptor on human erythrocytes. ACS nano. 2010; 4: 4609-20.
4. Rusu M DA, Curaj A, Liehn EA. Ultra-rapid non-invasive clinical nano-diagnostic of inflammatory diseases. Discoveries Reports. 2014; 1.
5. Muller DJ, Dufrene YF. Atomic force microscopy as a multifunctional molecular toolbox in nanobiotechnology. Nature nanotechnology. 2008; 3: 261-9.
6. Legleiter J, Czilli DL, Gitter B, DeMattos RB, Holtzman DM, Kowalewski T. Effect of different anti-Abeta antibodies on Abeta fibrillogenesis as assessed by atomic force microscopy. J Mol Biol. 2004; 335: 997-1006.
7. Ambre RNJAH. Overview literature on atomic force microscopy (AFM): Basics and its important applications for polymer characterization. Indian Journal of Engineering & Materials Sciences. 2006; 13: 368-84.
8. Iturri J, Toca-Herrera JL. Characterization of cell scaffolds by atomic force microscopy. Polymers. 2017; 9.
9. Levental KR, Yu H, Kass L, Lakins JN, Egeblad M, Erler JT, et al. Matrix crosslinking forces tumor progression by enhancing integrin signaling. Cell. 2009; 139: 891-906.
10. Cross SE, Jin YS, Rao J, Gimzewski JK. Nanomechanical analysis of cells from cancer patients. Nature nanotechnology. 2007; 2: 780-3.
11. McKnight AL, Kugel JL, Rossman PJ, Manduca A, Hartmann LC, Ehman RL. MR elastography of breast cancer: preliminary results. AJR American journal of roentgenology. 2002; 178: 1411-7.
12. Bercoff J, Chaffai S, Tanter M, Sandrin L, Catheline S, Fink M, et al. In vivo breast tumor detection using transient elastography. Ultrasound in medicine & biology. 2003; 29: 1387-96.
13. Vinckier A, Semenza G. Measuring elasticity of biological materials by atomic force microscopy. FEBS Lett. 1998; 430: 12-6.
14. Chang YR, Raghunathan VK, Garland SP, Morgan JT, Russell P, Murphy CJ. Automated AFM force curve analysis for determining elastic modulus of biomaterials and biological samples. J Mech Behav Biomed Mater. 2014; 37: 209-18.
15. Ding Y, Xu GK, Wang GF. On the determination of elastic moduli of cells by AFM based indentation. Sci Rep. 2017; 7: 45575.
16. Mahaffy RE, Park S, Gerde E, Kas J, Shih CK. Quantitative analysis of the viscoelastic properties of thin regions of fibroblasts using atomic force microscopy. Biophys J. 2004; 86: 1777-93.
17. Cavalcanti-Adam EA, Volberg T, Micoulet A, Kessler H, Geiger B, Spatz JP. Cell spreading and focal adhesion dynamics are regulated by spacing of integrin ligands. Biophysical journal. 2007; 92: 2964-74.
18. Trappmann B, Gautrot JE, Connelly JT, Strange DG, Li Y, Oyen ML, et al. Extracellular-matrix tethering regulates stem-cell fate. Nature materials. 2012; 11: 642-9.
19. Yijie Jiang KTT. Measurement of the strength and range of adhesion using atomic force microscopy. Extreme Mechanics Letters. 2016; 9: 119-26.
20. Ramakrishna SN, Clasohm LY, Rao A, Spencer ND. Controlling adhesion force by means of nanoscale surface roughness. Langmuir : the ACS journal of surfaces and colloids. 2011; 27: 9972-8.
21. Rijnaarts HHM, Norde W, Bouwer EJ, Lyklema J, Zehnder AJB. Reversibility and mechanism of bacterial adhesion. Colloids and Surfaces B: Biointerfaces. 1995; 4: 5-22.
22. Cuajungco MP, Goldstein LE, Nunomura A, Smith MA, Lim JT, Atwood CS, et al. Evidence that the beta-amyloid plaques of Alzheimer's disease represent the redox-silencing and entombment of abeta by zinc. The Journal of biological chemistry. 2000; 275: 19439-42.
23. Innocenti M, Salvietti E, Guidotti M, Casini A, Bellandi S, Foresti ML, et al. Trace copper(II) or zinc(II) ions drastically modify the aggregation behavior of amyloid-beta1-42: an AFM study. Journal of Alzheimer's disease : JAD. 2010; 19: 1323-9.
24. Hane FT, Hayes R, Lee BY, Leonenko Z. Effect of copper and zinc on the single molecule self-affinity of alzheimer's amyloid-β peptides. PLoS One. 2016; 11: e0147488-e.
25. Loskill P, Zeitz C, Grandthyll S, Thewes N, Müller F, Bischoff M, et al. Reduced adhesion of oral bacteria on hydroxyapatite by fluoride treatment. Langmuir : the ACS journal of surfaces and colloids. 2013; 29: 5528-33.
26. Fung CKM, Seiffert-Sinha K, Lai KWC, Yang R, Panyard D, Zhang J, et al. Investigation of human keratinocyte cell adhesion using atomic force microscopy. Nanomedicine : nanotechnology, biology, and medicine. 2010; 6: 191-200.
27. Zhang J, Abiraman K, Jones SM, Lykotrafitis G, Andemariam B. Regulation of active ICAM-4 on normal and sickle cell disease RBCs via AKAPs is revealed by AFM. Biophys J. 2017; 112: 143-52.
28. Merghni AK, Dorra K, Hentati H, et al. Quantification of Staphylococcus aureus adhesion forces on various dental restorative materials using atomic force microscopy. Appl Surf Sci. 2016; 379: 323-30.
29. Safenkova IV, Zherdev AV, Dzantievf BB. Application of atomic force microscopy for characteristics of single intermolecular interactions. Biochemistry Biokhimiia. 2012; 77: 1536-52.
30. Yeow N, Tabor RF, Garnier G. Mapping the distribution of specific antibody interaction forces on individual red blood cells. Scientific reports. 2017; 7: 41956.
31. Benoit M, Gabriel D, Gerisch G, Gaub HE. Discrete interactions in cell adhesion measured by single-molecule force spectroscopy. Nat Cell Biol. 2000; 2: 313-7.
32. Stroh CM, Ebner A, Geretschlager M, Freudenthaler G, Kienberger F, Kamruzzahan AS, et al. Simultaneous topography and recognition imaging using force microscopy. Biophys J. 2004; 87: 1981-90.
33. Lin L, Wang H, Liu Y, Yan H, Lindsay S. Recognition imaging with a DNA aptamer. Biophysical journal. 2006; 90: 4236-8.
34. Challa P. Genetics of pseudoexfoliation syndrome. Curr Opin Ophthalmol. 2009; 20: 88-91.
35. Rosenstein BJ, Zeitlin PL. Prognosis in cystic fibrosis. Curr Opin Pulm Med. 1995; 1: 444-9.
36. Kilgore PE, Salim AM, Zervos MJ, Schmitt HJ. Pertussis: microbiology, disease, treatment, and prevention. Clin Microbiol Rev. 2016; 29: 449-86.
37. Dugger BN, Dickson DW. Pathology of neurodegenerative diseases. Cold Spring Harb Perspect Biol. 2017; 9.
38. Bansode SB, Gacche RN. Glycation-induced modification of tissue-specific ECM proteins: A pathophysiological mechanism in degenerative diseases. Biochimica et biophysica acta General subjects. 2019; 1863: 129411.
39. Theocharis AD, Theocharis DA, De Luca G, Hjerpe A, Karamanos NK. Compositional and structural alterations of chondroitin and dermatan sulfates during the progression of atherosclerosis and aneurysmal dilatation of the human abdominal aorta. Biochimie. 2002; 84: 667-74.
40. Lynch M, Barallobre-Barreiro J, Jahangiri M, Mayr M. Vascular proteomics in metabolic and cardiovascular diseases. J Intern Med. 2016; 280: 325-38.

41. Fogel O, Richard-Miceli C, Tost J. Chapter Six - Epigenetic changes in chronic inflammatory diseases. In: Donev R, editor. Adv Protein Chem Struct Biol: Academic Press; 2017. p. 139-89.
42. Li Y, Lu L, Li J. Topological structures and membrane nanostructures of erythrocytes after splenectomy in hereditary spherocytosis patients via atomic force microscopy. Cell Biochem Biophys. 2016; 74: 365-71.
43. Zhang Y, Zhang W, Wang S, Wang C, Xie J, Chen X, et al. Detection of erythrocytes in patient with iron deficiency anemia using atomic force microscopy. Scanning. 2012; 34: 215-20.
44. Maciaszek JL, Lykotrafitis G. Sickle cell trait human erythrocytes are significantly stiffer than normal. J Biomech. 2011; 44: 657-61.
45. Jin H, Xing X, Zhao H, Chen Y, Huang X, Ma S, et al. Detection of erythrocytes influenced by aging and type 2 diabetes using atomic force microscope. Biochem Biophys Res Commun. 2010; 391: 1698-702.
46. Ebner A, Nikova D, Lange T, Haberle J, Falk S, Dubbers A, et al. Determination of CFTR densities in erythrocyte plasma membranes using recognition imaging. Nanotechnology. 2008; 19: 384017.
47. Zemla J, Stachura T, Gross-Sondej I, Gorka K, Okon K, Pyka-Fosciak G, et al. AFM-based nanomechanical characterization of bronchoscopic samples in asthma patients. J Mol Recognit. 2018; 31: e2752.
48. Hsieh CH, Lin YH, Lin S, Tsai-Wu JJ, Herbert Wu CH, Jiang CC. Surface ultrastructure and mechanical property of human chondrocyte revealed by atomic force microscopy. Osteoarthritis and cartilage. 2008; 16: 480-8.
49. Jin H, Liang Q, Chen T, Wang X. Resveratrol protects chondrocytes from apoptosis via altering the ultrastructural and biomechanical properties: an AFM study. PLoS One. 2014; 9: e91611.
50. Nagy N, de la Zerda A, Kaber G, Johnson PY, Hu KH, Kratochvil MJ, et al. Hyaluronan content governs tissue stiffness in pancreatic islet inflammation. J Biol Chem. 2018; 293: 567-78.
51. Creasey R, Sharma S, Craig JE, Gibson CT, Ebner A, Hinterdorfer P, et al. Detecting protein aggregates on untreated human tissue samples by atomic force microscopy recognition imaging. Biophys J. 2010; 99: 1660-7.
52. Nyongesa CO, Park S. Chemotherapeutic resistance: a nano-mechanical point of view. Biol Chem. 2018; 399: 1433-46.
53. W. Haberle JKHH, and G. Binnig. Force microscopy on living cells. American Vacuum Society. 1991; 9.
54. Jembrek MJ, Simic G, Hof PR, Segota S. Atomic force microscopy as an advanced tool in neuroscience. Transl Neurosci. 2015; 6: 117-30.
55. Dufrene YF. Atomic force microscopy, a powerful tool in microbiology. J Bacteriol. 2002; 184: 5205-13.
56. Li M, Liu LQ, Xi N, et al. Progress of AFM single-cell and single-molecule morphology imaging. Chin Sci Bull. 2013; 58: 3177-82.
57. Puvaneswary S, Balaji Raghavendran HR, Ibrahim NS, Murali MR, Merican AM, Kamarul T. A comparative study on morphochemical properties and osteogenic cell differentiation within bone graft and coral graft culture systems. Int J Med Sci. 2013; 10: 1608-14.
58. Henderson E, Haydon PG, Sakaguchi DS. Actin filament dynamics in living glial cells imaged by atomic force microscopy. Science. 1992; 257: 1944-6.
59. Jung SH, Park D, Park JH, Kim YM, Ha KS. Molecular imaging of membrane proteins and microfilaments using atomic force microscopy. Exp Mol Med. 2010; 42: 597-605.
60. Liu F, Burgess J, Mizukami H, Ostafin A. Sample preparation and imaging of erythrocyte cytoskeleton with the atomic force microscopy. Cell Biochem Biophys. 2003; 38: 251-70.
61. Masuda T, Xu X, Dimitriadis EK, Lahusen T, Deng CX. "DNA Binding Region" of BRCA1 affects genetic stability through modulating the Intra-S-Phase checkpoint. Int J Biol Sci. 2016; 12: 133-43.
62. Gallagher PG. Abnormalities of the erythrocyte membrane. Pediatr Clin North Am. 2013; 60: 1349-62.
63. Bain BJ. 5 - Blood cell morphology in health and disease. In: Bain BJ, Bates I, Laffan MA, editors. Dacie and Lewis Practical Haematology (Twelfth Edition): Elsevier; 2017. p. 61-92.
64. Bolton-Maggs PH, Stevens RF, Dodd NJ, Lamont G, Tittensor P, King MJ. Guidelines for the diagnosis and management of hereditary spherocytosis. Br J Haematol. 2004; 126: 455-74.
65. Cascio MJ, DeLoughery TG. Anemia: evaluation and diagnostic tests. Med Clin North Am. 2017; 101: 263-84.
66. Wilson ML. Laboratory diagnosis of malaria: conventional and rapid diagnostic methods. Arch Pathol Lab Med. 2013; 137: 805-11.
67. Zhu A, Kaneshiro M, Kaunitz JD. Evaluation and treatment of iron deficiency anemia: a gastroenterological perspective. Dig Dis Sci. 2010; 55: 548-59.
68. Poschl B, Waneesorn J, Thekisoe O, Chutipongvivate S, Karanis P. Comparative diagnosis of malaria infections by microscopy, nested PCR, and LAMP in northern Thailand. Am J Trop Med Hyg. 2010; 83: 56-60.
69. Liu L, Viel A, Le Saux G, Plawinski L, Muggiolu G, Barberet P, et al. Remote imaging of single cell 3D morphology with ultrafast coherent phonons and their resonance harmonics. Sci Rep. 2019; 9: 6409.
70. Murray CK, Gasser RA, Jr., Magill AJ, Miller RS. Update on rapid diagnostic testing for malaria. Clin Microbiol Rev. 2008; 21: 97-110.
71. Berhane A, Russom M, Bahta I, Hagos F, Ghirmai M, Uqubay S. Rapid diagnostic tests failing to detect Plasmodium falciparum infections in Eritrea: an investigation of reported false negative RDT results. Malar J. 2017; 16: 105.
72. Mohandas N, An X. Malaria and human red blood cells. Med Microbiol Immunol. 2012; 201: 593-8.
73. Autino B, Corbett Y, Castelli F, Taramelli D. Pathogenesis of malaria in tissues and blood. Mediterr J Hematol Infect Dis. 2012; 4: e2012061.
74. Aingaran M, Zhang R, Law SK, Peng Z, Undisz A, Meyer E, et al. Host cell deformability is linked to transmission in the human malaria parasite Plasmodium falciparum. Cell Microbiol. 2012; 14: 983-93.
75. Moxon CA, Grau GE, Craig AG. Malaria: modification of the red blood cell and consequences in the human host. Br J Haematol. 2011; 154: 670-9.
76. Eaton P, Zuzarte-Luis V, Mota MM, Santos NC, Prudencio M. Infection by Plasmodium changes shape and stiffness of hepatic cells. Nanomedicine. 2012; 8: 17-9.
77. Shi H, Liu Z, Li A, Yin J, Chong AG, Tan KS, et al. Life cycle-dependent cytoskeletal modifications in Plasmodium falciparum infected erythrocytes. PLoS One. 2013; 8: e61170.
78. Dearnley M, Chu T, Zhang Y, Looker O, Huang C, Klonis N, et al. Reversible host cell remodeling underpins deformability changes in malaria parasite sexual blood stages. Proc Natl Acad Sci U S A. 2016; 113: 4800-5.
79. Haberle W, Horber JK, Ohnesorge F, Smith DP, Binnig G. In situ investigations of single living cells infected by viruses. Ultramicroscopy. 1992; 42-44 (Pt B): 1161-7.
80. Ando T, Kodera N, Takai E, Maruyama D, Saito K, Toda A. A high-speed atomic force microscope for studying biological macromolecules. Proc Natl Acad Sci U S A. 2001; 98: 12468-72.
81. Kodera N, Yamamoto D, Ishikawa R, Ando T. Video imaging of walking myosin V by high-speed atomic force microscopy. Nature. 2010; 468: 72-6.
82. Watanabe H, Uchihashi T, Kobashi T, Shibata M, Nishiyama J, Yasuda R, et al. Wide-area scanner for high-speed atomic force microscopy. Rev Sci Instrum. 2013; 84: 053702.
83. Watanabe-Nakayama T, Ono K, Itami M, Takahashi R, Teplow DB, Yamada M. High-speed atomic force microscopy reveals structural dynamics of amyloid beta1-42 aggregates. Proc Natl Acad Sci U S A. 2016; 113: 5835-40.
84. Weissmann C. The state of the prion. Nat Rev Microbiol. 2004; 2: 861-71.
85. Aguzzi A, Heikenwalder M, Polymenidou M. Insights into prion strains and neurotoxicity. Nat Rev Mol Cell Biol. 2007; 8: 552-61.
86. Mead S, Reilly MM. A new prion disease: relationship with central and peripheral amyloidoses. Nat Rev Neurol. 2015; 11: 90-7.
87. Prusiner SB. Prions. Proc Natl Acad Sci U S A. 1998; 95: 13363-83.
88. Goedert M. Alpha-synuclein and neurodegenerative diseases. Nat Rev Neurosci. 2001; 2: 492-501.
89. Lee HJ, Bae EJ, Lee SJ. Extracellular alpha--synuclein-a novel and crucial factor in Lewy body diseases. Nat Rev Neurol. 2014; 10: 92-8.
90. Irwin DJ, Lee VM, Trojanowski JQ. Parkinson's disease dementia: convergence of alpha-synuclein, tau and amyloid-beta pathologies. Nat Rev Neurosci. 2013; 14: 626-36.
91. Maries E, Dass B, Collier TJ, Kordower JH, Steece-Collier K. The role of alpha-synuclein in Parkinson's disease: insights from animal models. Nat Rev Neurosci. 2003; 4: 727-38.
92. Cattaneo E, Zuccato C, Tartari M. Normal huntingtin function: an alternative approach to Huntington's disease. Nat Rev Neurosci. 2005; 6: 919-30.
93. Williams A. Defining neurodegenerative diseases. BMJ. 2002; 324: 1465-6.
94. Villemagne VL, Pike KE, Chetelat G, Ellis KA, Mulligan RS, Bourgeat P, et al. Longitudinal assessment of Abeta and cognition in aging and Alzheimer disease. Ann Neurol. 2011; 69: 181-92.
95. Shibata-Seki T, Tajima K, Takahashi H, Seki H, Masai J, Goto H, et al. AFM characterization of chemically treated corneal cells. Anal Bioanal Chem. 2015; 407: 2631-5.
96. Figuereido I, Paiotta A, Dal Magro R, Tinelli F, Corti R, Re F, et al. A new approach for glyco-functionalization of collagen-based biomaterials. Int J Mol Sci. 2019; 20.
97. Fantner GE, Barbero RJ, Gray DS, Belcher AM. Kinetics of antimicrobial peptide activity measured on individual bacterial cells using high-speed atomic force microscopy. Nature nanotechnology. 2010; 5: 280-5.
98. D'Agostino DP, Olson JE, Dean JB. Acute hyperoxia increases lipid peroxidation and induces plasma membrane blebbing in human U87 glioblastoma cells. Neuroscience. 2009; 159: 1011-22.
99. Sherratt MJ. Tissue elasticity and the ageing elastic fibre. Age (Dordr). 2009; 31: 305-25.
100. Lu P, Takai K, Weaver VM, Werb Z. Extracellular matrix degradation and remodeling in development and disease. Cold Spring Harb Perspect Biol. 2011; 3.
101. Guz N, Dokukin M, Kalaparthi V, Sokolov I. If cell mechanics can be described by elastic modulus: study of different models and probes used in indentation experiments. Biophys J. 2014; 107: 564-75.
102. Remmerbach TW, Wottawah F, Dietrich J, Lincoln B, Wittekind C, Guck J. Oral cancer diagnosis by mechanical phenotyping. Cancer Res. 2009; 69: 1728-32.
103. Schulze C, Wetzel F, Kueper T, Malsen A, Muhr G, Jaspers S, et al. Stiffening of human skin fibroblasts with age. Clinics in plastic surgery. 2012; 39: 9-20.
104. Schulze C, Wetzel F, Kueper T, Malsen A, Muhr G, Jaspers S, et al. Stiffening of human skin fibroblasts with age. Biophysical journal. 2010; 99: 2434-42.
105. Guck J, Schinkinger S, Lincoln B, Wottawah F, Ebert S, Romeyke M, et al. Optical deformability as an inherent cell marker for testing malignant transformation and metastatic competence. Biophysical journal. 2005; 88: 3689-98.
106. Guevorkian K, Maitre JL. Micropipette aspiration: A unique tool for exploring cell and tissue mechanics in vivo. Methods Cell Biol. 2017; 139: 187-201.

107. Hu S, Liu G, Chen W, Li X, Lu W, Lam RH, et al. Multiparametric biomechanical and biochemical phenotypic profiling of single cancer cells using an elasticity microcytometer. Small (Weinheim an der Bergstrasse, Germany). 2016; 12: 2300-11.
108. Pittman M, Chen Y. 3D-printed magnetic tweezers for dorsal traction force measurement. Biotechniques. 2018; 65: 347-9.
109. Kriegel F, Ermann N, Lipfert J. Probing the mechanical properties, conformational changes, and interactions of nucleic acids with magnetic tweezers. J Struct Biol. 2017; 197: 26-36.
110. Long X, Parks JW, Stone MD. Integrated magnetic tweezers and single-molecule FRET for investigating the mechanical properties of nucleic acid. Methods. 2016; 105: 16-25.
111. Zhou Z, Zheng C, Li S, Zhou X, Liu Z, He Q, et al. AFM nanoindentation detection of the elastic modulus of tongue squamous carcinoma cells with different metastatic potentials. Nanomedicine. 2013; 9: 864-74.
112. Park S, Lee YJ. Nano-mechanical compliance of Muller cells investigated by atomic force microscopy. Int J Biol Sci. 2013; 9: 702-6.
113. Lee YJ, Patel D, Park S. Local rheology of human neutrophils investigated using atomic force microscopy. Int J Biol Sci. 2011; 7: 102-11.
114. Yamagishi A, Susaki M, Takano Y, Mizusawa M, Mishima M, Iijima M, et al. The structural function of nestin in cell body softening is correlated with cancer cell metastasis. Int J Biol Sci. 2019; 15: 1546-56.
115. Park S, Koch D, Cardenas R, Kas J, Shih CK. Cell motility and local viscoelasticity of fibroblasts. Biophysical journal. 2005; 89: 4330-42.
116. Schillers H, Rianna C, Schape J, Luque T, Doschke H, Walte M, et al. Standardized nanomechanical atomic force microscopy procedure (SNAP) for measuring soft and biological samples. Scientific reports. 2017; 7: 5117.
117. Webb HK, Truong VK, Hasan J, Crawford RJ, Ivanova EP. Physico-mechanical characterisation of cells using atomic force microscopy - Current research and methodologies. Journal of microbiological methods. 2011; 86: 131-9.
118. Park S, Bastatas L, Matthews J, Lee YJ. Mechanical responses of cancer cells on nanoscaffolds for adhesion size control. Macromolecular bioscience. 2015; 15: 851-60.
119. Akhtar R, Graham HK, Derby B, Sherratt MJ, Trafford AW, Chadwick RS, et al. Frequency-modulated atomic force microscopy localises viscoelastic remodelling in the ageing sheep aorta. J Mech Behav Biomed Mater. 2016; 64: 10-7.
120. Plodinec M, Loparic M, Monnier CA, Obermann EC, Zanetti-Dallenbach R, Oertle P, et al. The nanomechanical signature of breast cancer. Nature nanotechnology. 2012; 7: 757-65.
121. Shen J, Xie Y, Liu Z, Zhang S, Wang Y, Jia L, et al. Increased myocardial stiffness activates cardiac microvascular endothelial cell via VEGF paracrine signaling in cardiac hypertrophy. J Mol Cell Cardiol. 2018; 122: 140-51.
122. Martin JA, Buckwalter JA. Aging, articular cartilage chondrocyte senescence and osteoarthritis. Biogerontology. 2002; 3: 257-64.
123. Kim HT, Lo MY, Pillarisetty R. Chondrocyte apoptosis following intraarticular fracture in humans. Osteoarthritis Cartilage. 2002; 10: 747-9.
124. Loening AM, James IE, Levenston ME, Badger AM, Frank EH, Kurz B, et al. Injurious mechanical compression of bovine articular cartilage induces chondrocyte apoptosis. Arch Biochem Biophys. 2000; 381: 205-12.
125. Stolz M, Gottardi R, Raiteri R, Miot S, Martin I, Imer R, et al. Early detection of aging cartilage and osteoarthritis in mice and patient samples using atomic force microscopy. Nature nanotechnology. 2009; 4: 186-92.
126. Mauad T, Xavier AC, Saldiva PH, Dolhnikoff M. Elastosis and fragmentation of fibers of the elastic system in fatal asthma. Am J Respir Crit Care Med. 1999; 160: 968-75.
127. Williamson JP, McLaughlin RA, Noffsinger WJ, James AL, Baker VA, Curatolo A, et al. Elastic properties of the central airways in obstructive lung diseases measured using anatomical optical coherence tomography. Am J Respir Crit Care Med. 2011; 183: 612-9.
128. Kol N, Shi Y, Tsvitov M, Barlam D, Shneck RZ, Kay MS, et al. A stiffness switch in human immunodeficiency virus. Biophys J. 2007; 92: 1777-83.
129. Magdesian MH, Sanchez FS, Lopez M, Thostrup P, Durisic N, Belkaid W, et al. Atomic force microscopy reveals important differences in axonal resistance to injury. Biophys J. 2012; 103: 405-14.
130. Spedden E, White JD, Naumova EN, Kaplan DL, Staii C. Elasticity maps of living neurons measured by combined fluorescence and atomic force microscopy. Biophysical journal. 2012; 103: 868-77.
131. Martin M, Benzina O, Szabo V, Vegh AG, Lucas O, Cloitre T, et al. Morphology and nanomechanics of sensory neurons growth cones following peripheral nerve injury. PLoS One. 2013; 8: e56286.
132. Huang S, Ingber DE. The structural and mechanical complexity of cell-growth control. Nat Cell Biol. 1999; 1: E131-8.
133. Gumbiner BM. Cell adhesion: the molecular basis of tissue architecture and morphogenesis. Cell. 1996; 84: 345-57.
134. Szekanecz Z, Koch AE. Cell-cell interactions in synovitis. Endothelial cells and immune cell migration. Arthritis Res. 2000; 2: 368-73.
135. Helenius J, Heisenberg CP, Gaub HE, Muller DJ. Single-cell force spectroscopy. J Cell Sci. 2008; 121: 1785-91.
136. Guedes AF, Carvalho FA, Moreira C, Nogueira JB, Santos NC. Essential arterial hypertension patients present higher cell adhesion forces, contributing to fibrinogen-dependent cardiovascular risk. Nanoscale. 2017; 9: 14897-906.
137. Khalili AA, Ahmad MR. A review of cell adhesion studies for biomedical and biological applications. Int J Mol Sci. 2015; 16: 18149-84.
138. Yu M, Strohmeyer N, Wang J, Muller DJ, Helenius J. Increasing throughput of AFM-based single cell adhesion measurements through multisubstrate surfaces. Beilstein J Nanotechnol. 2015; 6: 157-66.
139. Christ KV, Turner KT. Methods to measure the strength of cell adhesion to substrates. J Adhes Sci Technol. 2010; 24: 37-41.
140. Yamamoto A, Mishima S, Maruyama N, Sumita M. Quantitative evaluation of cell attachment to glass, polystyrene, and fibronectin- or collagen-coated polystyrene by measurement of cell adhesive shear force and cell detachment energy. J Biomed Mater Res. 2000; 50: 114-24.
141. Puech PH, Taubenberger A, Ulrich F, Krieg M, Muller DJ, Heisenberg CP. Measuring cell adhesion forces of primary gastrulating cells from zebrafish using atomic force microscopy. J Cell Sci. 2005; 118: 4199-206.
142. Loskill P, Zeitz C, Grandthyll S, Thewes N, Muller F, Bischoff M, et al. Reduced adhesion of oral bacteria on hydroxyapatite by fluoride treatment. Langmuir : the ACS journal of surfaces and colloids. 2013; 29: 5528-33.
143. Loesche WJ. Microbiology of dental decay and periodontal disease. In: Baron S, ed. Medical Microbiology, 4th ed. Galveston (TX): University of Texas Medical Branch at Galveston; 1996: 99.
144. Anees A Siddiqui SAS, Suhail Ahmad, Seemi Siddiqui, Iftikhar Ahsan, Kapendra Sahu Diabetes: mechanism, pathophysiology and management-A review. International Journal of Drug Development and Research. 2013; 5(2): 1-23.
145. Skyler JS, Bakris GL, Bonifacio E, Darsow T, Eckel RH, Groop L, et al. Differentiation of diabetes by pathophysiology, Natural History, and Prognosis. Diabetes. 2017; 66: 241-55.
146. Wu Y, Ding Y, Tanaka Y, Zhang W. Risk factors contributing to type 2 diabetes and recent advances in the treatment and prevention. Int J Med Sci. 2014; 11: 1185-200.
147. Swagerty DL, Jr., Hellinger D. Radiographic assessment of osteoarthritis. Am Fam Physician. 2001; 64: 279-86.
148. Braun HJ, Gold GE. Diagnosis of osteoarthritis: imaging. Bone. 2012; 51: 278-88.
149. Kellgren JH, Lawrence JS. Radiological assessment of osteo-arthrosis. Ann Rheum Dis. 1957; 16: 494-502.
150. Altman R, Asch E, Bloch D, Bole G, Borenstein D, Brandt K, et al. Development of criteria for the classification and reporting of osteoarthritis. Classification of osteoarthritis of the knee. Diagnostic and Therapeutic Criteria Committee of the American Rheumatism Association. Arthritis Rheum. 1986; 29: 1039-49.
151. Spector TD, Hart DJ, Byrne J, Harris PA, Dacre JE, Doyle DV. Definition of osteoarthritis of the knee for epidemiological studies. Ann Rheum Dis. 1993; 52: 790-4.
152. Chen A, Balogun-Lynch J, Aggarwal K, Dick E, Gupte CM. Should all elective knee radiographs requested by general practitioners be performed weight-bearing? Springerplus. 2014; 3: 707.
153. Crockett-Torabi E, Ward PA. The role of leukocytes in tissue injury. European journal of anaesthesiology. 1996; 13: 235-46.
154. Jaczewska J, Abdulreda MH, Yau CY, Schmitt MM, Schubert I, Berggren PO, et al. TNF-alpha and IFN-gamma promote lymphocyte adhesion to endothelial junctional regions facilitating transendothelial migration. J Leukoc Biol. 2014; 95: 265-74.
155. Fung CK, Seiffert-Sinha K, Lai KW, Yang R, Panyard D, Zhang J, et al. Investigation of human keratinocyte cell adhesion using atomic force microscopy. Nanomedicine : nanotechnology, biology, and medicine. 2010; 6: 191-200.
156. Hane FT, Hayes R, Lee BY, Leonenko Z. Effect of copper and zinc on the single molecule self-affinity of alzheimer's amyloid-beta peptides. PloS one. 2016; 11: e0147488.
157. Fletcher DA, Mullins RD. Cell mechanics and the cytoskeleton. Nature. 2010; 463: 485-92.
158. Xu L, Josan JS, Vagner J, Caplan MR, Hruby VJ, Mash EA, et al. Heterobivalent ligands target cell-surface receptor combinations in vivo. Proc Natl Acad Sci U S A. 2012; 109: 21295-300.
159. Dupres V, Alsteens D, Wilk S, Hansen B, Heinisch JJ, Dufrene YF. The yeast Wsc1 cell surface sensor behaves like a nanospring in vivo. Nat Chem Biol. 2009; 5: 857-62.
160. Li M. LL, Xi N., Wang Y. Progress in measuring biophysical properties of membrane proteins with AFM single-molecule force spectroscopy. Chin Sci Bull. 2014; 59: 2717–25.
161. Fernandez-Leiro R, Scheres SH. Unravelling biological macromolecules with cryo-electron microscopy. Nature. 2016; 537: 339-46.
162. Betzig E, Patterson GH, Sougrat R, Lindwasser OW, Olenych S, Bonifacino JS, et al. Imaging intracellular fluorescent proteins at nanometer resolution. Science. 2006; 313: 1642-5.
163. Rambo RP, Tainer JA. Super-resolution in solution X-ray scattering and its applications to structural systems biology. Annu Rev Biophys. 2013; 42: 415-41.
164. Ebner A, Kienberger F, Kada G, Stroh CM, Geretschlager M, Kamruzzahan AS, et al. Localization of single avidin-biotin interactions using simultaneous topography and molecular recognition imaging. Chemphyschem. 2005; 6: 897-900.
165. Anderson NL, Anderson NG. The human plasma proteome: history, character, and diagnostic prospects. Molecular & cellular proteomics : MCP. 2002; 1: 845-67.
166. Wilson R. Sensitivity and specificity: twin goals of proteomics assays. Can they be combined? Expert review of proteomics. 2013; 10: 135-49.

167. Ott W, Jobst MA, Schoeler C, Gaub HE, Nash MA. Single-molecule force spectroscopy on polyproteins and receptor-ligand complexes: The current toolbox. Journal of structural biology. 2017; 197: 3-12.
168. Kienberger F, Ebner A, Gruber HJ, Hinterdorfer P. Molecular recognition imaging and force spectroscopy of single biomolecules. Accounts of chemical research. 2006; 39: 29-36.
169. Bukharina NS, Ivanov YD, Pleshakova TO, Frantsuzov PA, Andreeva EY, Kaysheva AL, et al. [Atomic force microscopy fishing of gp120 on immobilized aptamer and its mass spectrometry identification]. Biomeditsinskaia khimiia. 2015; 61: 363-72.
170. Allison DP, Hinterdorfer P, Han W. Biomolecular force measurements and the atomic force microscope. Curr Opin Biotechnol. 2002; 13: 47-51.
171. Senapati S, Manna S, Lindsay S, Zhang P. Application of catalyst-free click reactions in attaching affinity molecules to tips of atomic force microscopy for detection of protein biomarkers. Langmuir : the ACS journal of surfaces and colloids. 2013; 29: 14622-30.
172. Braunstein GM, Roman RM, Clancy JP, Kudlow BA, Taylor AL, Shylonsky VG, et al. Cystic fibrosis transmembrane conductance regulator facilitates ATP release by stimulating a separate ATP release channel for autocrine control of cell volume regulation. J Biol Chem. 2001; 276: 6621-30.
173. Sheppard DN, Welsh MJ. Structure and function of the CFTR chloride channel. Physiol Rev. 1999; 79: S23-45.
174. Vankeerberghen A, Cuppens H, Cassiman JJ. The cystic fibrosis transmembrane conductance regulator: an intriguing protein with pleiotropic functions. J Cyst Fibros. 2002; 1: 13-29.
175. Kalin N, Claass A, Sommer M, Puchelle E, Tummler B. DeltaF508 CFTR protein expression in tissues from patients with cystic fibrosis. J Clin Invest. 1999; 103: 1379-89.
176. Dupuit F, Kalin N, Brezillon S, Hinnrasky J, Tummler B, Puchelle E. CFTR and differentiation markers expression in non-CF and delta F 508 homozygous CF nasal epithelium. J Clin Invest. 1995; 96: 1601-11.
177. Servidoni MF, Gomez CCS, Marson FAL, Toro A, Ribeiro M, Ribeiro JD, et al. Sweat test and cystic fibrosis: overview of test performance at public and private centers in the state of Sao Paulo, Brazil. J Bras Pneumol. 2017; 43: 121-8.
178. Bennekou P. K+-valinomycin and chloride conductance of the human red cell membrane. Influence of the membrane protonophore carbonylcyanide m-chlorophenylhydrazone. Biochim Biophys Acta. 1984; 776: 1-9.
179. Raftos JE, Bookchin RM, Lew VL. Distribution of chloride permeabilities in normal human red cells. J Physiol. 1996; 491 (Pt 3): 773-7.
180. Dvorak-Theobald G. Pseudoexfoliation of the lens capsule: relation to true exfoliation of the lens capsule as reported in the literature, and role in the production of glaucoma capsulocuticulare. Trans Am Ophthalmol Soc. 1953; 51: 385-407.
181. Lee RK. The molecular pathophysiology of pseudoexfoliation glaucoma. Curr Opin Ophthalmol. 2008; 19: 95-101.
182. Dewundara S, Pasquale LR. Exfoliation syndrome: a disease with an environmental component. Curr Opin Ophthalmol. 2015; 26: 78-81.
183. Anastasopoulos E, Founti P, Topouzis F. Update on pseudoexfoliation syndrome pathogenesis and associations with intraocular pressure, glaucoma and systemic diseases. Curr Opin Ophthalmol. 2015; 26: 82-9.
184. Ahmed IK. The Art of Managing PXF Glaucoma. Review of Opthalmology. 2012.
185. Clark CG, Sun Z, Meininger GA, Potts JT. Atomic force microscopy to characterize binding properties of alpha7-containing nicotinic acetylcholine receptors on neurokinin-1 receptor-expressing medullary respiratory neurons. Exp Physiol. 2013; 98: 415-24.
186. Cordero-Erausquin M, Marubio LM, Klink R, Changeux JP. Nicotinic receptor function: new perspectives from knockout mice. Trends Pharmacol Sci. 2000; 21: 211-7.
187. Cohen G, Roux JC, Grailhe R, Malcolm G, Changeux JP, Lagercrantz H. Perinatal exposure to nicotine causes deficits associated with a loss of nicotinic receptor function. Proc Natl Acad Sci U S A. 2005; 102: 3817-21.
188. Melvin JA, Scheller EV, Miller JF, Cotter PA. Bordetella pertussis pathogenesis: current and future challenges. Nat Rev Microbiol. 2014; 12: 274-88.
189. Liu DF, Phillips E, Wizemann TM, Siegel MM, Tabei K, Cowell JL, et al. Characterization of a recombinant fragment that contains a carbohydrate recognition domain of the filamentous hemagglutinin. Infect Immun. 1997; 65: 3465-8.
190. Mielcarek N, Riveau G, Remoue F, Antoine R, Capron A, Locht C. Homologous and heterologous protection after single intranasal administration of live attenuated recombinant Bordetella pertussis. Nat Biotechnol. 1998; 16: 454-7.
191. Van der Zee A, Schellekens JF, Mooi FR. Laboratory diagnosis of pertussis. Clin Microbiol Rev. 2015; 28: 1005-26.
192. Arnal L, Longo G, Stupar P, Castez MF, Cattelan N, Salvarezza RC, et al. Localization of adhesins on the surface of a pathogenic bacterial envelope through atomic force microscopy. Nanoscale. 2015; 7: 17563-72.